Available online at www.sciencedirect.com

ScienceDirect

Ceramics International 40 (2014) 2305–2313

CERAMICS INTERNATIONAL

www.elsevier.com/locate/ceramint

A study on in-situ synthesis of TiB_2–SiC ceramic composites by reactive hot pressing

Guolong Zhao[a,b], Chuanzhen Huang[a,b,*], Hanlian Liu[a,b], Bin Zou[a,b], Hongtao Zhu[a,b], Jun Wang[a,b]

[a]*Centre for Advanced Jet Engineering Technologies (CaJET), School of Mechanical Engineering, Shandong University, Jinan 250061, PR China*
[b]*Key Laboratory of High-efficiency and Clean Mechanical Manufacture (Shandong University), Ministry of Education, PR China*

Received 23 May 2013; received in revised form 19 July 2013; accepted 31 July 2013
Available online 7 August 2013

Abstract

TiB_2–SiC ceramic composites with (10–20) wt% SiC were in-situ synthesized by the reactive hot pressing (RHP) process at 1700 °C under 32 MPa in vacuum. The influence of SiC content and sintering time on the microstructure and mechanical properties of the composites was investigated in detail. The fracture toughness increased while the flexural strength and hardness decreased as the content of SiC increased. Elongated TiB_2 grains with a diameter of 1–2 μm and an aspect ratio of 3–6 were in-situ synthesized in the composites. The composite containing 15 wt% SiC had the optimum comprehensive mechanical properties with flexural strength of 704 MPa, fracture toughness of 5.6 MPa $m^{1/2}$ and hardness of 19.8 GPa. The improved mechanical properties were attributed to the mixed fracture mode, the strengthening and toughening mechanisms of SiC particles and elongated TiB_2 grains including crack bridging, crack deflection, crack branching, grain fracture and the interlocking structure. The fracture toughness and hardness increased due to the improved relative density and higher yield of elongated TiB_2 grains as the sintering time increased. However, the abnormal grain growth deteriorated the flexural strength when the sintering time further increased.

Keywords: B. Composites; C. Mechanical properties; D. SiC; Reactive hot pressing

1. Introduction

As one of the transition metal borides, titanium diboride (TiB_2) has received wide attention because of its high melting point, high hardness and elastic modulus, great chemical stability as well as good thermal and electrical conductivity. This combination of properties makes it to be a candidate material for high temperature structural applications such as cutting tools, seals, armor and crucibles. However, the densification of the monolithic TiB_2 ceramics is difficult because of its high melting point, low self-diffusion coefficient and the comparatively high vapor pressure of the constituent [1]. The application of the monolithic TiB_2 ceramics is still restricted by its low sinterability, poor mechanical properties and oxidation resistance at above 1000 °C. Generally, the densification of monolithic TiB_2 ceramics is proceeded at high temperatures (> 2000 °C) under a high applied pressure. Nevertheless, the high temperatures result in exaggerated grain growth which is detrimental to the mechanical properties. Up to now, the flexural strength and fracture toughness of the monolithic TiB_2 ceramics prepared by the hot pressing process and pressureless sintering method are 360–450 MPa and 3.3–5.0 MPa $m^{1/2}$ respectively, which are inadequate to many applications.

Much progress has been achieved in improving the sinterability and mechanical properties of TiB_2 ceramics in recent years. Metallic sintering additives such as nickel, cobalt, iron and chromium have been used to reduce the sintering temperature and promote the densification of TiB_2 ceramics through the hot pressing and pressureless sintering processes [2,3]. Ferber et al. [4] fabricated TiB_2 ceramics containing 0–10 wt% Ni by hot pressing and found that the highest flexural strength and fracture toughness (670 MPa and 6.4 MPa $m^{1/2}$ respectively) were obtained when only 1.4 wt% Ni was added. However, the high-temperature mechanical properties of the TiB_2 ceramics will be decreased dramatically by the presence

*Corresponding author at: Centre for Advanced Jet Engineering Technologies (CaJET), School of Mechanical Engineering, Shandong University, Jinan 250061, PR China. Tel./fax: +86 531 88396913.
E-mail address: chuanzhenh@sdu.edu.cn (C. Huang).

0272-8842/$ - see front matter © 2013 Elsevier Ltd and Techna Group S.r.l. All rights reserved.
http://dx.doi.org/10.1016/j.ceramint.2013.07.152

of metallic additives because of their softening effect at elevated temperatures. Melendez-Martinez et al. [5] studied the high temperature mechanical properties of ZrB_2–4 wt% Ni and found that the presence of Ni dominated the fracture behavior and was responsible for the dramatic strength degradation. A combination of high hardness and fracture toughness is obtainable with the use of an appropriate amount of non-metallic sintering additives. Various non-metallic sintering additives such as AlN [6], Si_3N_4 [7], TiC [8] and $MoSi_2$ [9,10] have been applied to improve the oxidation resistance and mechanical properties of TiB_2 ceramics. Among them, SiC is an appropriate candidate for improving the sinterability and mechanical properties of TiB_2 ceramics. Traditionally, the TiB_2–SiC ceramic composites were prepared by the hot pressing and hot isostatic pressing method. Torizuka et al. [11] prepared the TiB_2 ceramics with 2.5 wt% SiC as additive and 96% of the theoretical density was achieved by the hot pressing (HP) process and a density of 99% was achieved by the hot isostatic pressing (HIP) process. However, the grain and pore coarsening were promoted by the oxide (mainly TiO_2 and B_2O_3) which is usually present on the surface of the commercial TiB_2 powder [12] and the maximum attainable density was limited. In addition, the fracture toughness (4.3 MPa $m^{1/2}$) was low and the cost was relatively high. As an in-situ technique, reactive hot pressing (RHP) is a promising process to in-situ synthesize the secondary phase in the ceramic matrix directly. Compared with the conventional process, RHP has the advantages of low cost, low sintering temperature, clean interfaces between the component phases, etc. In addition, the microstructure and mechanical properties of the ceramics prepared by the RHP process can be tailored. Up to now, very few reports on in-situ synthesis of TiB_2–SiC ceramic composite by reactive hot pressing can be noted.

In this work, TiB_2–SiC ceramic composites with different contents of SiC were in-situ synthesized by the reactive hot pressing process at 1700 °C under 32 MPa. The influence of SiC content and sintering time on the microstructure and mechanical properties of the composites was investigated. The composites were analyzed by the observation of scanning electron microscope (SEM), energy dispersive spectrometer (EDS) and X-ray diffraction (XRD).

2. Experimental procedure

The TiB_2–SiC ceramic composites were prepared by the reactive hot pressing process according to the following reaction:

$$Si + 2Ti + B_4C + xTiB_2 \rightarrow (2 + x)TiB_2 + SiC \quad (1)$$

where x is the amount of TiB_2 powder (mol) used as the raw material. The starting powders were Si, Ti, B_4C and TiB_2 and their characteristics provided by the suppliers are listed in Table 1. The TiB_2 raw powder was firstly ball-milled in ethanol medium using tungsten carbide (WC) balls for 72 h in order to crush big powder particles, and then the powder was dried in a vacuum dry oven. The stoichiometric powders according to Table 2 were mixed and ball-milled using analytical-grade ethanol as the medium with WC balls for 48 h in polyethylene jars. After dried and sieved through a 120-mesh sieve, the mixture was placed into a graphite die and then reactive hot pressed at 1700 °C under a pressure of 32 MPa in vacuum. A heating rate of 50 °C/min was employed. The obtained compact was plate with about 42 mm in diameter and 4.5 mm in thickness.

The reactive hot pressed compacts were cut into mechanical property testing bars with a dimension of 3 mm × 4 mm × 30 mm using electro-discharge machining tool and the surfaces of the testing bars were polished using polishing machinery with diamond slurries. The edges of all the testing bars were chamfered to minimize the stress concentration induced during the machining process. The flexural strength of the composites was measured in the static air using a three-point bending tester (WDW-50E) with a span of 20 mm and a loading rate of 0.5 mm/min according to Chinese National Standards GBT6569-2006 [13] and the load was applied parallel to the reactive hot pressing direction. The Vickers hardness was measured on the polished surface using a Vickers diamond pyramid indenter (HVS-50) with a static load of 196 N and a loading duration time of 15 s according to Chinese National Standards GB/T16534-2009 [14]. The values of the fracture toughness (K_{IC}) were calculated by the equation reported by Fukuhara et al. [15] considering an average of ten specimens:

$$K_{IC} = 0.203 H_V a^{1/2} \left[\frac{c}{a}\right]^{-3/2} \quad (2)$$

where, H_V is the Vickers hardness, $2a$ is the length of the impression diagonal and $2c$ is the overall indentation crack length including $2a$. The relative density of each specimen was measured by the Archimedes method with deionized water as the medium. At least 15 specimens were tested for each experimental condition.

The phase identification of the composites was carried out by an X-ray diffraction (XRD) (Hitachi RAX-10A-X). $CuK_{\alpha 1}$ radiation ($\lambda = 1.54050$ Å) and a scan step of 10°/min were used. The XRD peaks were identified by matching to the JCPDS-ICDD data cards. The microstructure, propagation of the indentation cracks and the chemical constituent of the composites were investigated by a scanning electron microscopy (SEM) (ZEISS SUPRA55) equipped with an energy-dispersive spectrometer (EDS) (ACT-350).

3. Results and discussion

3.1. Phase identification

The TiB_2–SiC ceramic composites with different contents of SiC can be prepared by changing the value of x in reaction (1), indicating that the microstructure of the composites can be tailored via the reactive hot pressing process. It was seen from Table 2 that the mass fraction of TiB_2 in the composites was higher than that of SiC, so TiB_2 and SiC can be treated as the matrix and the secondary-phase particles respectively in the present work. The XRD patterns of TS10, TS15 and TS20 are shown in Fig. 1. TiB_2–SiC ceramic composites were successfully in-situ synthesized by the reactive hot pressing process. In this work, the TiB_2 powder that was used as the raw

material had a diluting effect on the reaction among Si, Ti and B_4C. However, except for TiB_2 and SiC, no other phases were detected by the XRD patterns shown in Fig. 1, indicating that no significant influences of the raw TiB_2 powder on the synthesis of TiB_2–SiC were found and a full conversion of reagents into products was achieved.

Table 1
Characteristics of the starting powders.

Powder	Purity	Particle size (μm)	Supplier
Si	99.9%	1.0	Shanghai st-nano science and technology Co., Ltd.
Ti	99.5%	45.0	General research institute for nonferrous metals
B_4C	99.0%	7.0	Jingangzuan boron carbide Co., Ltd.
TiB_2	98.5%	1.3	Ningxia Machinery Research Institute Co., Ltd.

Table 2
Composition ratio of TiB_2–SiC ceramic composites.

Symbol	x Value	Composition ratio (wt%)	
		TiB_2	SiC
TS10	3.1936	90	10
TS15	1.2701	85	15
TS20	0.3083	80	20

3.2. Effect of SiC content on the microstructure and mechanical properties

The flexural strength, fracture toughness and Vickers hardness of the composites are shown in Fig. 2. It was indicated that the SiC content had great influence on the mechanical properties of the composites. When the content of SiC increased, the fracture toughness increased while both the flexural strength and hardness decreased. The composite containing 15 wt% SiC (TS15) had the optimum comprehensive mechanical properties with flexural strength of 704 MPa, fracture toughness of 5.6 MPa $m^{1/2}$ and hardness of 19.8 GPa. SEM micrographs on the fractured surfaces of TS10, TS15 and TS20 synthesized at 1700 °C for 30 min are shown in Fig. 3.

The EDS analysis shown in Fig. 4 indicated that the fine grains and the coarse grains shown in Fig. 3(a) were SiC and TiB_2 respectively. It could be seen that the grain size of the in-situ synthesized SiC was 0.5–1 μm and that of TiB_2 was 2–5 μm, indicating that ceramic composite with fine microstructure could be synthesized by the reactive hot pressing process using starting powders with larger particle size. As shown in Fig. 3(a), SiC grains were distributed uniformly in the interspaces among the large TiB_2 grains and few pores were observed, which resulted in a higher relative density. Additionally, different from the weak TiB_2–SiC interface of the composite fabricated by the hot pressing or pressureless sintering process, the interface between the in-situ synthesized TiB_2 and SiC was "clean" and free from any interfacial phase [16]. As a result, the flexural strength and hardness of

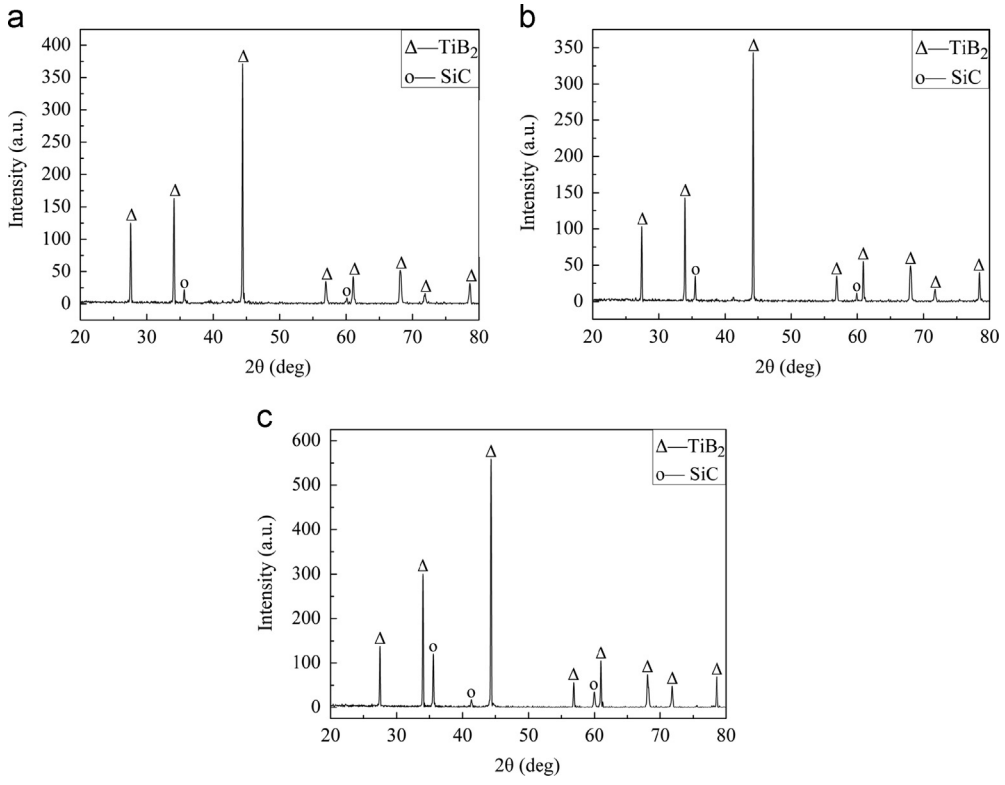

Fig. 1. XRD patterns of (a) TS10, (b) TS15 and (c) TS20.

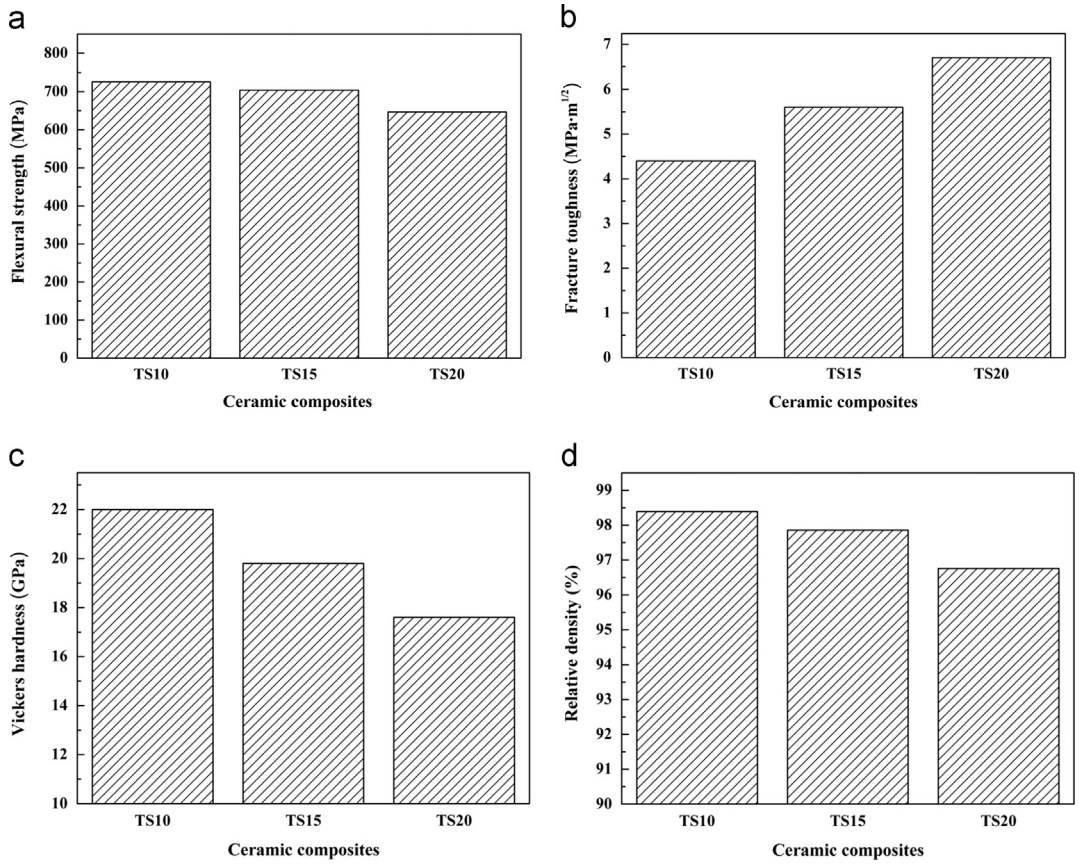

Fig. 2. Mechanical properties of the composites: (a) flexural strength, (b) fracture toughness and (c) Vickers hardness.

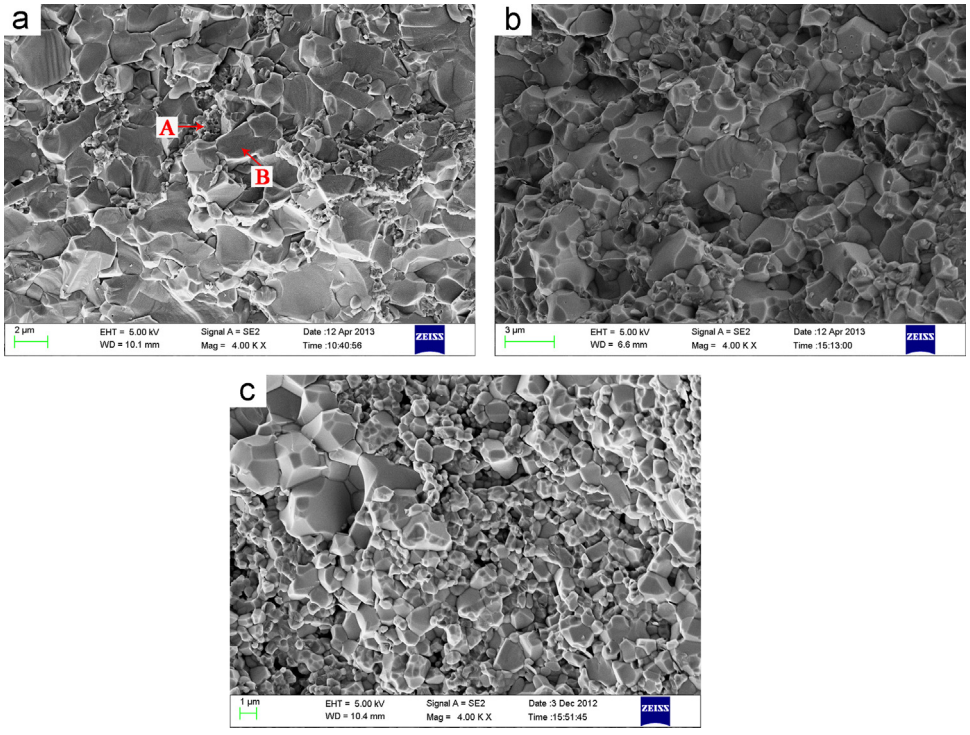

Fig. 3. SEM micrographs on the fractured surfaces of (a) TS10, (b) TS15 and (c) TS20 synthesized at 1700 °C for 30 min.

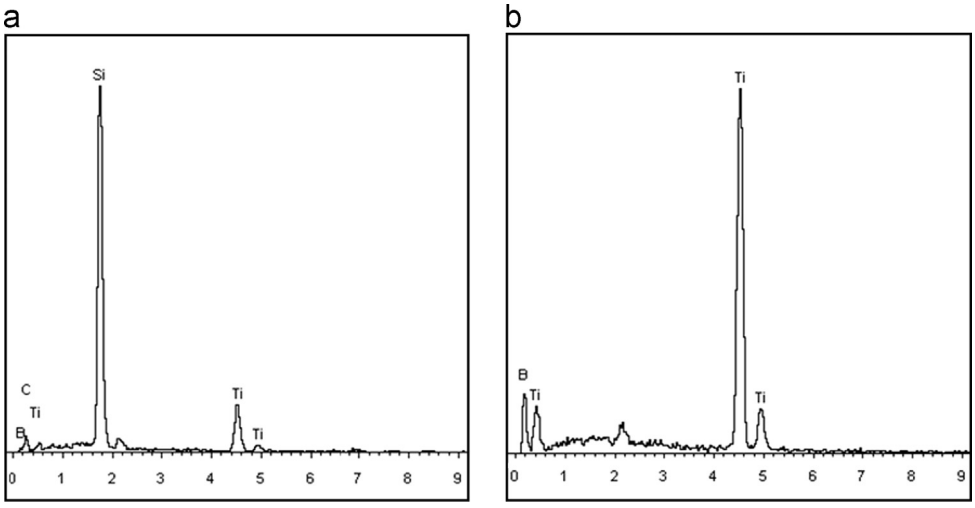

Fig. 4. EDS patterns for (a) point A and (b) point B in Fig. 3(a).

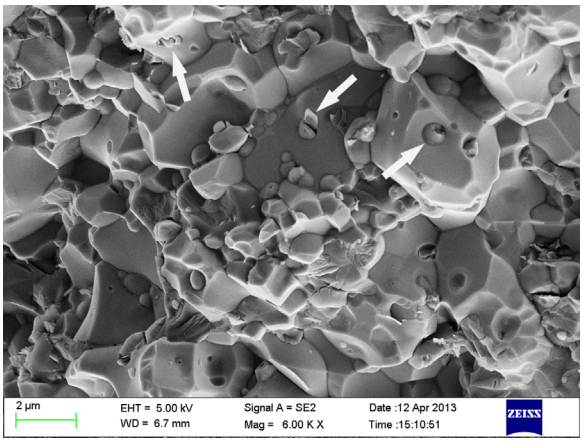

Fig. 5. SEM micrograph on the distribution of SiC in TS15.

the composite were improved. However, the fracture mode of TS10 was the single transgranular fracture and almost no intergranular fracture feature was observed. It is seen from Fig. 3(b) that the fracture surface of TS15 was characterized by a mixed mode of intergranular and transgranular fracture, presenting a more complicated fracture mode, which led to the improved mechanical properties. In addition, as shown in Fig. 5, the SiC grains were not only distributed in the interspaces among the large TiB_2 grains, but also embedded in the TiB_2 grains, as denoted by the arrows. As a result, the SiC particulate bridging was easily created and the crack surfaces were pinned together effectively, thereby increasing the resistance to crack extension. According to the crack bridging toughening mechanism demonstrated by Becher [17], the relatively higher fracture toughness was obtained. The great fracture toughness of TS20 was attributed to the toughening effects of the elongated TiB_2 grains, which will be discussed in the following part. However, the partial agglomeration of coarse TiB_2 grains was observed in TS20 shown in Fig. 3(c), thus leading to the low flexural strength. In addition, pores were also distributed among the grains and the relative density was decreased, as a result, the hardness of TS20 was decreased.

The SEM micrographs on the polished surfaces of the composites synthesized at 1700 °C for 30 min are shown in Fig. 6. Different amounts of elongated grains were randomly oriented and uniformly distributed in the composites. The elongated grains were 1–2 μm in diameter and 3–6 in aspect ratio. The EDS analysis in Fig. 7 revealed that the elongated grain shown in Fig. 6(a) was TiB_2. The white phase shown in Fig. 6(a) was WC that scrapped off from the WC balls during the ball milling process, which will be discussed in the following part. Fig. 6(a–c) demonstrates that the content of SiC had a significant effect on the microstructure of the composites, especially on the yield of the elongated TiB_2 grains. It was seen that the volume fraction of the elongated TiB_2 grains increased as the content of SiC increased from 10 wt% to 20 wt%. As illustrated in Fig. 8, the toughening mechanisms of the elongated TiB_2 grains were considered as crack deflection, crack branching, grain bridging and grain fracture. When the front of the crack encountered the elongated TiB_2 grains with high elastic modulus, the grain-matrix interface debonding tended to occur and the crack was deflected to propagate through a more tortuous path as shown in Fig. 8(a). Thus additional fracture energy was consumed and the fracture toughness was improved. The mismatch of thermal expansion coefficient between TiB_2 (4.6×10^{-6}/°C) and SiC (4.02×10^{-6}/°C) resulted in the residual tensile stress on the matrix and compressive stress on the secondary-phase particles, which enhanced the generation of micro-cracks [18]. The crack branching was enhanced by these micro-cracks when the main crack propagated as shown in Fig. 8(b). As a result, more fracture energy was dissipated and the crack extension was impeded, thus leading to the improved toughness. The crack bridging effect shown in Fig. 8(c) by an elongated TiB_2 grain provided a restraining force for the crack growth. Similar to the whisker fracture toughening mechanism illustrated in Ref. [19], the fracture of the elongated TiB_2 grain shown in Fig. 8(c) consumed fracture energy sharply during the crack propagation process, which resulted in the improved toughness. It could be seen from Fig. 6(c) that the interlocking structures (denoted by the circles) were generated since the elongated TiB_2 grains interconnected with each other. The interlocking structure was considered to greatly improve the damage tolerance of the composite [20]. However, pores were likely to be introduced by these interlocked

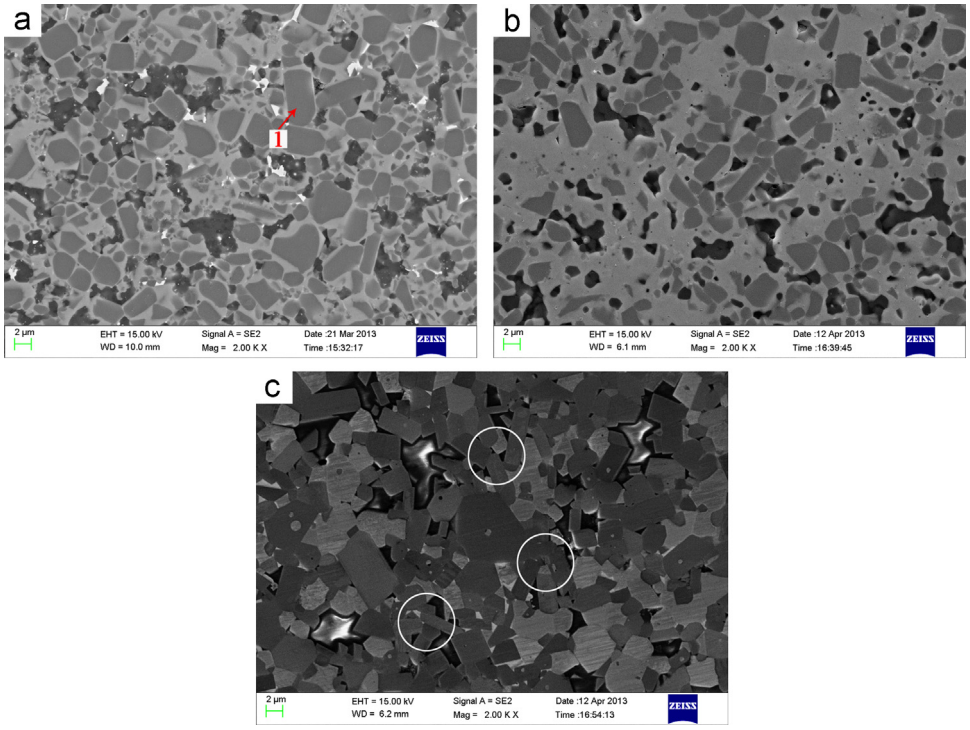

Fig. 6. SEM micrographs on the polished surfaces of (a) TS10, (b) TS15 and (c) TS20 synthesized at 1700 °C for 30 min.

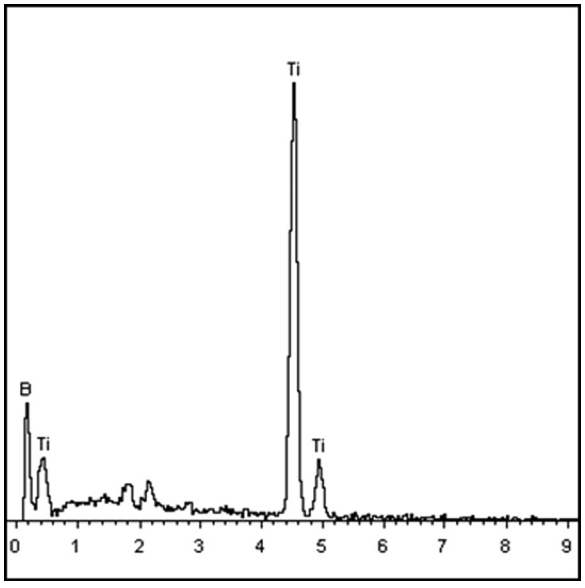

Fig. 7. EDS pattern for point 1 in Fig. 6(a).

elongated grains and the flexural strength was decreased. Therefore, the higher fracture toughness of TS20 was ascribed to the interaction of these effective fracture energy consuming mechanisms.

3.3. Effect of sintering time on the microstructure and mechanical properties

The effect of the sintering time on the mechanical properties of TS15 is shown in Fig. 9. It was seen that the flexural strength increased as the sintering time increased from 15 to 30 min while decreased with the further increase of the sintering time. Both the fracture toughness and the hardness of the composite increased gradually as the sintering time increased. The SEM micrographs on the fractured and polished surfaces of TS15 are shown in Figs. 10 and 11 respectively. The EDS analysis in Fig. 12 revealed that the white phase shown in Fig. 11(b) was WC. It was seen from Fig. 10(a) that when the sintering time was 15 min, the composite was not fully dense and pores existed at the grain boundaries. The pores weakened the grain boundaries and would play as the origin of cracks if the composite was exposed to external load. In addition, only a few of the elongated TiB_2 grains were synthesized when the sintering time was 15 min and a small amount of coarse grains were produced as shown in Figs. 10 and 11(a). As a result, the mechanical properties of the composite were decreased. When the sintering time was 45 min, a higher density was achieved and the fracture mode of the composite was a mixture of intergranular and transgranular fracture, indicating that the pore was an important factor that influenced the fracture mode of the composite. As shown in Fig. 11(b), the yield of the elongated TiB_2 grains increased as the sintering time increased, indicating that a long sintering time was suitable for the growth of the elongated grains and beneficial to the fracture toughness of the composite. However, increasing the sintering time resulted in the abnormal grain growth of SiC, which was detrimental to the flexural strength of the composite.

4. Conclusions

(1) The TiB_2–SiC ceramic composites with different contents of SiC were in-situ synthesized by the reactive hot pressing (RHP) process at 1700 °C under 32 MPa in vacuum. The composition identified by an X-ray diffraction (XRD)

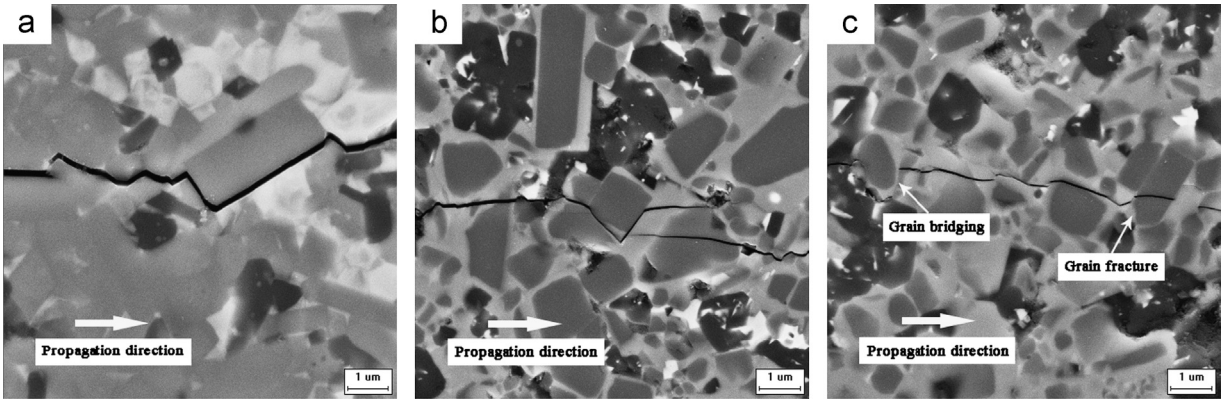

Fig. 8. SEM micrographs of (a) crack deflection, (b) crack branching and (c) grain bridging and grain fracture of TS20 synthesized at 1700 °C for 30 min.

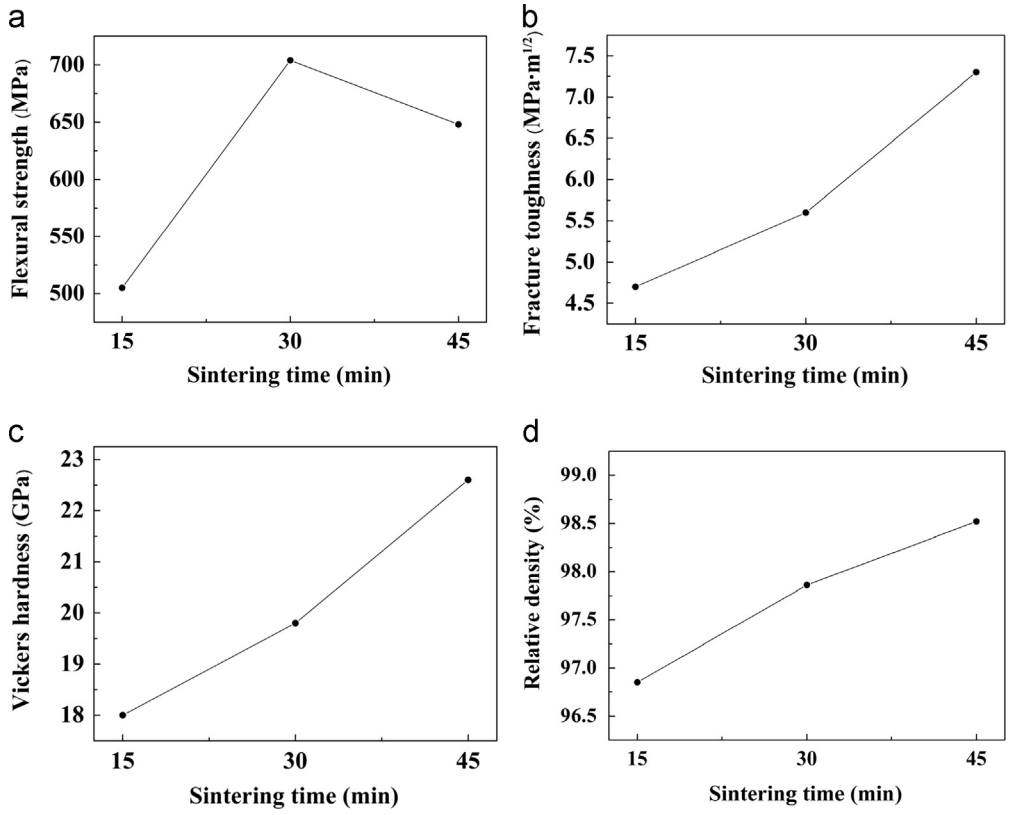

Fig. 9. Effect of sintering time on the (a) flexural strength, (b) fracture toughness and (c) Vickers hardness of TS15.

indicated a full conversion of reagents into products was achieved. The influence of SiC content and sintering time on the microstructure and mechanical properties of the composites was investigated by a scanning electron microscope (SEM) equipped with an energy dispersive spectrometer (EDS).

(2) The content of SiC had a significant influence on the microstructure and mechanical properties of the composites. Elongated TiB_2 grains with a diameter of 1–2 μm and an aspect ratio of 3–6 were in-situ synthesized in the composites. The composite containing 15 wt% SiC (TS15) had the optimum comprehensive mechanical properties with flexural strength of 704 MPa, fracture toughness of 5.6 MPa $m^{1/2}$ and hardness of 19.8 GPa. The improved mechanical properties were attributed to the mixed mode of intergranular and transgranular fracture, the strengthening and toughening effects of SiC particles and elongated TiB_2 grains including crack bridging, crack deflection, crack branching, grain fracture and the interlocking structure.

(3) The sintering time had a significant influence on the microstructure and mechanical properties of the composites. The yield of the elongated TiB_2 grains and the relative density of the composites increased with an increase in the sintering time, which resulted in improved fracture toughness and hardness. However, the flexural strength was decreased

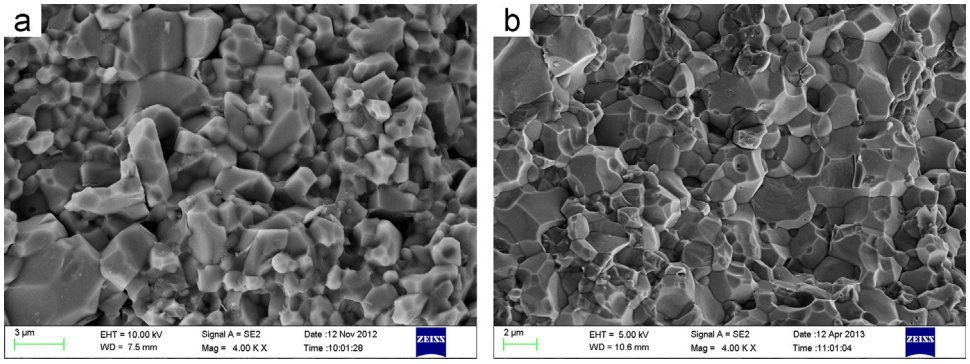

Fig. 10. SEM micrographs on the fractured surfaces of TS15 sintered for (a) 15 min and (b) 45 min.

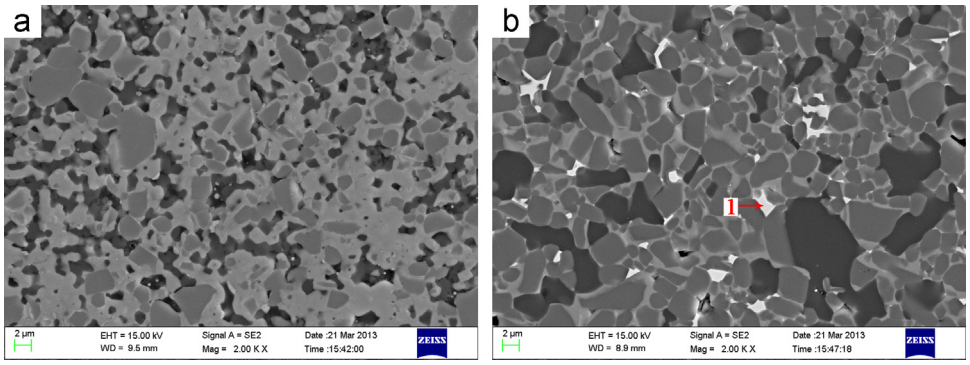

Fig. 11. SEM micrographs on the polished surfaces of TS15 sintered for (a) 15 min and (b) 45 min.

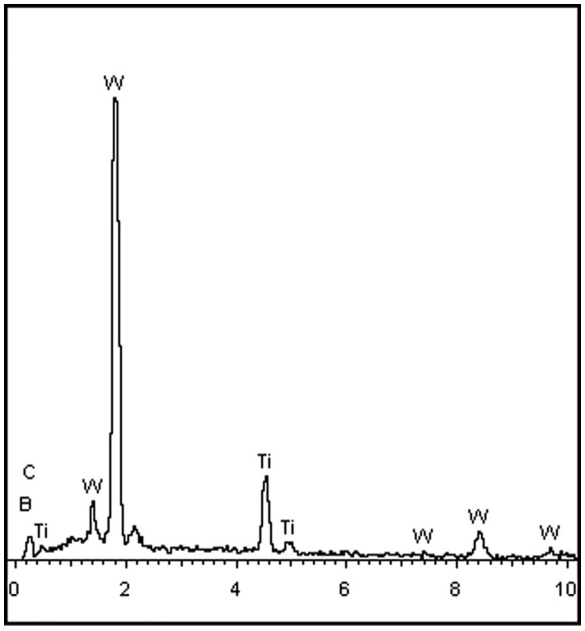

Fig. 12. EDS pattern for point 1 in Fig. 11(b).

due to the abnormal grain growth when the sintering time further increased.

Acknowledgments

The work is supported by Key Special Project of Numerical Control Machine Tool (2012ZX04003-051).

References

[1] B. Basu, G.B. Raju, A.K. Suri, Processing and properties of monolithic TiB_2 based materials, International Materials Reviews 51 (2006) 352–374.
[2] M.A. Einarsrud, E. Hagen, G. Pettersen, T. Grande, Pressureless sintering of titanium diboride with nickel, nickel boride, and iron additives, Journal of the American Ceramic Society 80 (1997) 3013–3020.
[3] S.H. Kang, D.J. Kim, E.S. Kang, S.S. Baek, Pressureless sintering and properties of titanium diboride ceramics containing chromium and iron, Journal of the American Ceramic Society 84 (2001) 893–895.
[4] M.K. Ferber, P.F. Becher, C.B. Finch, Effect of microstructure on the properties of TiB_2 ceramics, Journal of the American Ceramic Society (1983) 2–4.
[5] J.J. Melendez-Martinez, A. Dominguez-Rodriguez, F. Monteverde, C. Melandri, G. Portu, Characterisation and high temperature mechanical properties of zirconium boride-based materials, Journal of the European Ceramic Society 22 (2002) 2543–2549.
[6] L.H. Li, H.E. Kim, E.S. Kang, Sintering and mechanical properties of titanium diboride with aluminum nitride as a sintering aid, Journal of the European Ceramic Society 22 (2002) 973–977.
[7] J.H. Park, Y.H. Koh, H.E. Kim, C.S. Hwang, Densification and mechanical properties of titanium deboride with silicon nitride as a sintering aid, Journal of the American Ceramic Society 82 (1999) 3037–3042.
[8] S.K. Bhaumik, C. Divakar, A.K. Singh, G.S. Upadhyaya, Synthesis and sintering of TiB_2 and TiB_2–TiC composite under high pressure, Materials Science and Engineering: A 279 (2000) 275–281.
[9] T.S.R.Ch. Murthy, B. Basu, R. Balasubramaniam, Processing and properties of TiB_2 with $MoSi_2$ sinter-additive: a first report, Journal of the American Ceramic Society 89 (2006) 131–138.
[10] K. Biswas, B. Basu, A.K. Suri, K. Chattopadhyay, A TEM study on TiB_2–10% $MoSi_2$ composite: microstructure development and densification mechanism, Scripta Materialia 54 (2006) 1363–1368.

[11] S. Torizuka, K. Sato, H. Nishio, T. Kishi, Effect of SiC on interfacial reaction and sintering mechanism of TiB_2, Journal of the American Ceramic Society 78 (1995) 1606–1610.
[12] S. Baik, P.F. Becher, Effect of oxygen contamination on densification of TiB_2, Journal of the American Ceramic Society 70 (1987) 527–530.
[13] China State Bureau of Technological Supervision, Chinese national standards-test method for flexural strength of monolithic ceramics at room temperature, Chinese Standard Publishing House, Beijing, 2006.
[14] China State Bureau of Technological Supervision, Chinese national standards-test method for hardness of monolithic ceramics at room temperature, Chinese Standard Publishing House, Beijing, 2009.
[15] M. Fukuhara, K. Fukazawa, A. Fukawa, Physical properties and cutting performance of silicon nitride ceramic, Wear 102 (1985) 195–210.
[16] G.J. Zhang, X.M. Yue, Z.Z. Jin, J.Y. Dai, In-situ synthesized TiB_2 toughened SiC, Journal of the European Ceramic Society 16 (1996) 409–412.
[17] P.F. Becher, Microstructural design of toughened ceramics, Journal of the American Ceramic Society 74 (1991) 255–269.
[18] M. Taya, S. Hayashi, A.S. Kobayashi, H.S. Yoon, Toughening of a particulate-reinforces ceramic-matrix composite by thermal residual stress, Journal of the American Ceramic Society 73 (1990) 1382–1391.
[19] G.L. Zhao, C.Z. Huang, H.L. Liu, B. Zou, H.T. Zhu, J. Wang, Preparation of in-situ growth TaC whiskers toughening Al_2O_3 ceramic matrix composite, International Journal of Refractory Metals and Hard Materials 36 (2013) 122–125.
[20] L. Xu, C.Z. Huang, H.L. Liu, B. Zou, H.T. Zhu, G.L. Zhao, J. Wang, In situ synthesis of ZrB_2–ZrC_x ceramic tool materials toughened by elongated ZrB_2 grains, Materials and Design 49 (2013) 226–233.